

Skeletal Phenotyping in Rodents: Tissue Isolation and Manipulation

2

Janet E. Henderson, Chan Gao, and Edward J. Harvey

2.1 Introduction

The pioneering work of Rudolph Jaenisch at the Whitehead Institute¹ and Mario Capecchi at the Howard Hughes Institute² used modification of the mouse genome to understand the etiology and pathogenesis of human disease. Their groundbreaking studies in the 1980s revealed the power of mouse genetic and genomic research and were the driving force behind the explosive growth of transgenic science as we know it today. Enormous resources have been expended in the academic and private sectors for vivaria to generate, breed, and house mice with targeted mutations in thousands of genes. Complicated breeding programs have been established to generate mice carrying compound mutations as well as recombinant congenic strains with known segments of one strain incorporated into the genome of another.³ The success of these genetic-based approaches using animal models to predict susceptibility or resistance to human disease relies heavily on the ability to accurately and reliably characterize the phenotypic traits associated with that disease.

Like the vast majority of common pathologies that affect human populations, osteoporosis is a complex, polygenic, and multifactorial disease that is characterized by a reduction in bone strength that predisposes it to fracture.⁴ Historically, bone mineral density (BMD) has been used as the principle surrogate marker of bone strength for the purpose of diagnosing

osteoporosis in human⁵ and mouse⁶ populations. BMD remains an important diagnostic tool and an indicator of response to treatment. Additional tests including biochemical markers of bone metabolism⁷ and noninvasive measurements of bone architecture using quantitative computed tomography (qCT) are also frequently used.⁸ Although genetic profiling for bone disease is still at an early stage of development, it is widely accepted that genetic background plays a significant role in determining individual differences in bone development and the rate and extent to which bone metabolism changes over time.⁹ Many of the genes that have been linked to osteopenic or osteoporotic phenotypes include components of growth factor, cytokine and steroid hormone-signaling pathways, and the major collagenous and non-collagenous bone matrix proteins.

Of primary importance in the selection of an appropriate animal model is its predictive value for use in the diagnosis or treatment of human disease. Mutations in osteoporosis-related genes in the mouse genome have produced remarkably similar phenotypes to those observed in humans, thus identifying these animals as a valuable resource to study the interplay between genetic and epigenetic factors in the pathogenesis of osteoporosis.¹⁰ Among the many advantages that mice have over other animal models commonly used to study bone disease are preexisting disease with a well-documented progression, a program of skeletal development similar to that seen in humans, relatively low cost and wide accessibility, a rapid breeding cycle and defined genetics, and, above all, established protocols for the phenotypic and molecular analysis of their skeleton. For these reasons, genetically modified mice remain the model of choice for the functional analysis of osteoporosis as well as other diseases. The comprehensive skeletal phenotyping protocol described in this

J.E. Henderson (✉)

Department of Medicine and Surgery, McGill University Health Centre, Montreal General Hospital, Room A5.169, 1650 Cedar Ave., Montreal, Québec H3G 1A4, Canada
e-mail: janet.henderson@mcgill.ca

chapter was developed for screening populations of mice arising from genetic recombination³ and chemical mutagenesis,^{11,12} and has been used with success to characterize the skeletons of mice with targeted genetic mutations.¹³⁻²¹

2.2 Primary Screen for a Skeletal Phenotype

The different steps in the primary skeletal screen can be performed rapidly and provide sufficient information to pinpoint heritable defects in trabecular and cortical bone that will impact on its functional properties. It is unlikely that the defects identified in a primary bone screen will resolve over time if the animals are phenotyped after 4 months of age when they are skeletally mature. The progressive nature of a comprehensive screen for a skeletal phenotype is illustrated in Fig. 2.1 along with examples of micro-computed tomography (μ CT) and histological analyses performed in the primary (1°) and secondary (2°) screens.

2.2.1 Genetic Background

A skeletal phenotype analysis begins with documentation of the genetic background of the mice. Similar genetic and gender-determined differences in bone traits, such as size, shape, and BMD are seen in humans and in inbred strains of mice. The Jackson Laboratory maintains a Mouse Phenome Database (<http://phenome.jax.org>), which is an excellent source of information on inbred strain differences in body composition, skeletal morphology, BMD, bone strength, and other criteria that could potentially impact on the overall skeletal phenotype. These inter-strain differences in bone have been exploited as a mechanism to localize disease genes to specific segments of the genome. An example is the AcB/BcA gene discovery platform consisting of 36 recombinant congenic strains (RCS) that were generated from an intercross between A/J and C57BL6J mouse strains to study susceptibility to infection.²² Subsequent backcross of the descendants for ten generations to

one or the other original strain, designated the recipient, resulted in the RCS carrying 12.5% of the donor genome in the recipient genome. Using BMD and μ CT as a screening tool, several RCS with 87.5% C57BL6J DNA exhibited reduced BMD compared with the parental strain. This indicated that low BMD, which is a characteristic of A/J mice, was conferred in the 12.5% of A/J DNA.³ Genetic mapping of this segment can then identify novel molecular targets for diagnostic or therapeutic interventions.

2.2.2 Age and Sex

In addition to the genetic background, the age and sex of the mouse can impact heavily on the bone phenotype. Skeletal maturity is attained between 4 and 5 months of age in mice and in most strains there are significant differences between males and females. The parameters that are commonly used to characterize the bone phenotype, including BMD, cortical width, trabecular volume, and architecture, change over time in much the same way as they do in growing children. It is therefore difficult to draw conclusions regarding the impact of a specific gene mutation from phenotypic analyses performed before 4 months, for instance in strains that are neonatally or perinatally lethal. Even when dealing with adult mice it is always good practice to consult with the Mouse Phenome Database to familiarize oneself with the expected skeletal phenotype of wild-type mice in the genetic background on which a mutation is bred. Some examples of work performed by investigators in collaboration with the Jackson Labs include mapping of genetic variability in BMD,²³ bone strength,²⁴ biomechanical properties,²⁵ and IGF-1 status,^{26,27} as well as genome-wide screening for mutations using advanced sequencing technologies.²⁸ Comparisons between C3H/HeJ and C57BL6J male and female mice revealed significantly greater BMD in the skull and lumbar vertebrae of C3H mice. The data came from five independent studies by four different investigators using two different technologies, dual x-ray absorptiometry (DXA) and peripheral quantitative computed tomography (pQCT). Striking differences in femoral cortical width and cross-sectional geometry were reflected in the differences in biomechanical strength, with the thinner cortex of C57BL6J mice conferring susceptibility

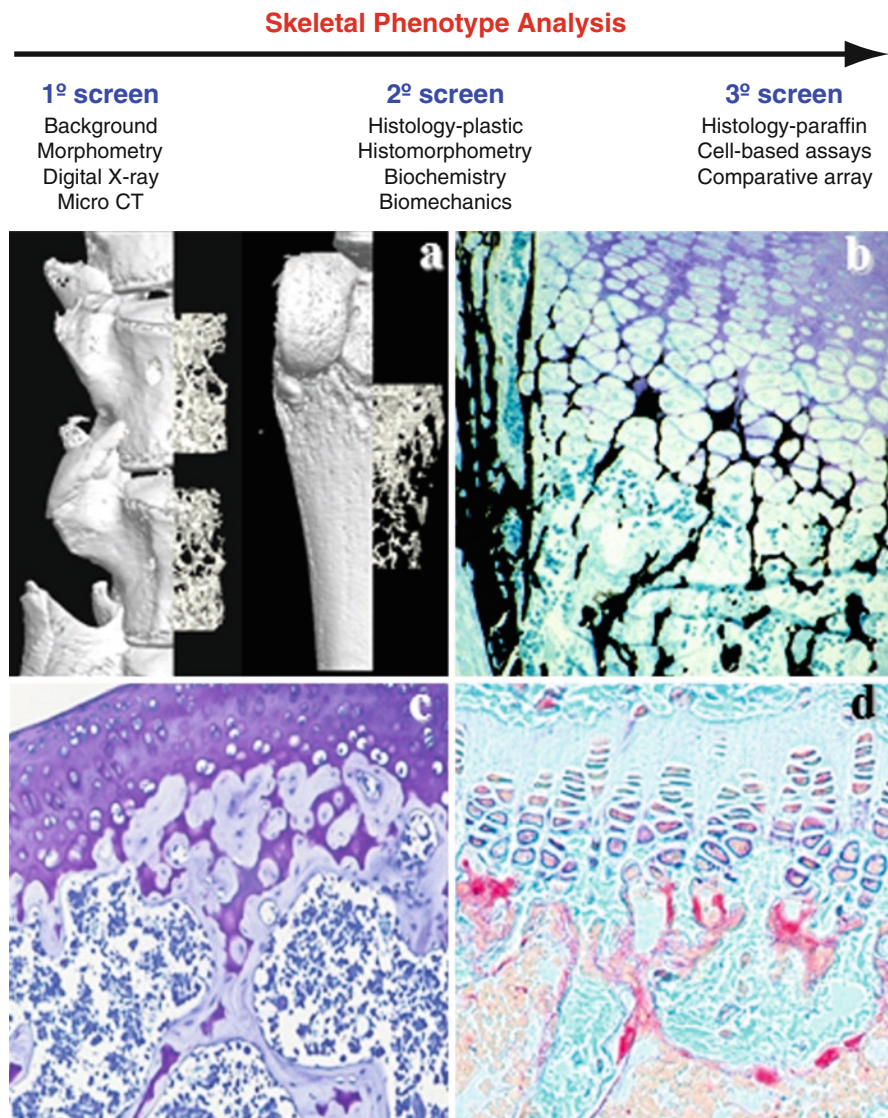


Fig. 2.1 Skeletal phenotype analysis through sequential screens. The skeleton is analyzed systematically and progressively for traits from the macroscopic to the molecular level through a series of screens. The primary (1°) screen provides information on the genetic background, the morphology of key skeletal elements, and analysis of bone architecture using μ CT (**a**). The secondary (2°) screen involves detailed histological analyses of plastic-embedded bone for mineral, osteoid, osteoblast, and osteoclast activity. (**b**) Details of the deposition of mineral (black) at the chondro-osseous junction of the growth plate, and

(**c**) the articular surface of a joint with metachromatic staining of mineralized cartilage cores (purple), and the bone that has been laid down by osteoblasts on top of them. (**d**) The chondro-osseous junction, with osteoblasts stained purple with ALP and osteoclasts stained red with TRAP. Immunochemical analyses of bone are not commonly performed and are thus placed in the tertiary (3°) screen along with detailed analyses of bone marrow-derived or limb bud MSC and gene- or protein-based comparative arrays to explore the molecular mechanisms

to fracture. Craniofacial morphology also differed, with the C3H mice exhibiting a shorter skull and nasal length and a deeper cranial vault than the C57BL6J strain. It is interesting to note that when mice homozygous for a null mutation of fibroblast growth factor

receptor 3 (FGFR3) were bred onto a C3H background to improve longevity¹⁵ the phenotype of the axial and appendicular skeleton was virtually identical to that seen on the C57BL/6 background.^{29,30} The dramatic improvement in their viability identified these mice as

a valuable resource to study skeletal aging and bone regeneration in mice with a heritable predisposition to osteomalacia and osteopenia.

2.2.3 Radiology

Once the pedigree and morphological features of the mouse have been documented it is time to perform radiological imaging of the skeleton. For a detailed discussion of animal imaging please refer to [Chap. 5](#) of this book. A dedicated small animal x-ray instrument like the XPert 80 (Kubtek, Milford CT) with a 50 kV, 1 mA source and digital capability is best suited to this task. Imaging for longitudinal studies is performed on mice lightly anesthetized for immobilization and at a magnification of up to 5 \times depending on the region of interest (ROI). This provides an electronic record of the gross skeletal phenotype for the measurement of skeletal elements, most commonly the femur, tibia, vertebra, and skull. To avoid difficulties associated with the transfer of animals in and out of a barrier facility any instrument to be used on live animals is best placed inside the barrier. For skeletal imaging this might include a DXA, a μ CT, and in rare cases a small animal magnetic resonance imaging MRI instrument for joint imaging. The gradual shift in emphasis from BMD alone in the clinical diagnosis of osteoporosis to a broader definition that involves bone architecture is reflected in a reduction in the use of DXA and an increase in μ CT in preclinical animal models. This has been enabled in part by a reduction in the cost of the instruments over the past decade and by improved technology for data processing and storage capabilities. In keeping with the focus of this chapter, the following discussion of μ CT imaging will be restricted to postmortem applications and from our experience using Skyscan (<http://www.skyscan.be>) instruments.

2.2.4 Terminal Procedures and Tissue Harvest

When euthanizing an animal for the purpose of characterizing its skeletal phenotype one should harvest body fluids for biochemical analyses along with the

skeletal elements from skull to tail. The time taken for terminal procedures should be recorded to ensure that processing of all tissues from the cohort being euthanized can be accomplished within 1 h of death. For large cohorts this is best accomplished by a team with each member assigned to a specific task from anesthesia, to blood letting, to tissue harvest. To avoid using expensive and time-consuming metabolic protocols for the collection of urine samples, the mouse can be placed on a cold glass plate and spot urine aspirated with a sterile micropipette. Whole blood removed by cardiac puncture from anesthetized animals is processed to obtain serum or plasma for biochemical analyses and, if needed, high molecular weight DNA can be isolated for genetic studies. The selection of bones for analysis should ensure consistency from one experiment to the next and to obtain the maximum information from a single animal. [Figure 2.2](#) shows an x-ray image with the allocation of different skeletal elements for a typical phenotyping experiment. It is time- and cost-effective to harvest everything even though some of the bones may not be used. All bones removed for μ CT are fixed overnight at 4°C in fresh 4% paraformaldehyde, rinsed in three exchanges of sterile phosphate buffered saline (PBS) and stored at 4°C in PBS until they are scanned. Using the pelvic girdle as a reference point the lumbar vertebrae are removed en bloc for μ CT and histological analysis and the thoracic vertebrae removed and frozen for micro-mechanical testing or RNA extraction if needed. Both femurs are carefully disarticulated from the pelvis and from the tibia at the knee, being extremely careful not to damage the articular surfaces or subchondral bone. Depending on the battery of tests that the investigator is interested in, the long bones are either fixed and scanned using μ CT prior to histological processing (see below) or frozen for biomechanical testing or RNA analyses. The skull is usually frozen for future reference unless the investigator has a particular interest in its analysis.¹⁸

2.2.5 Microcomputed Tomographic Imaging

There are an increasing number of institutions using desktop μ CT instruments for high-resolution three-dimensional

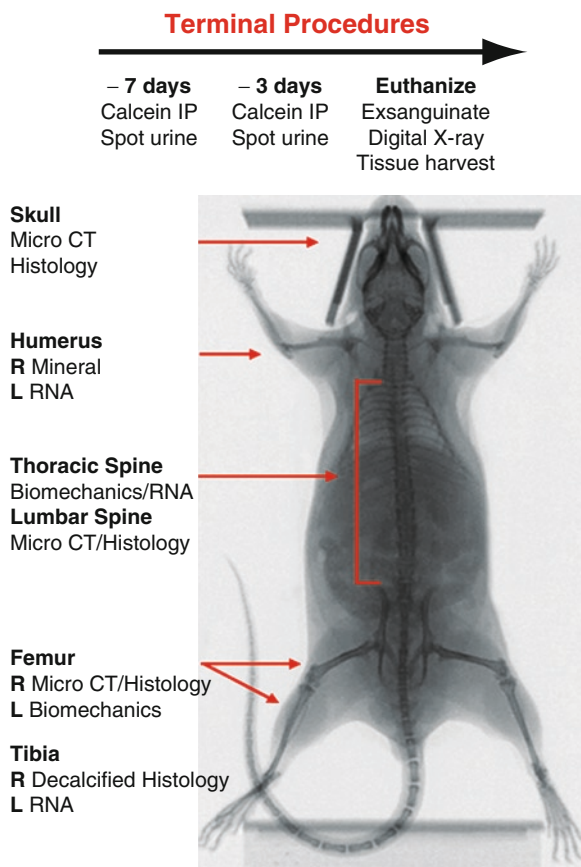


Fig. 2.2 Terminal procedures and bone harvest for skeletal phenotype. Seven days prior to euthanization young adult mice are first placed on a cold glass plate to induce voiding of the bladder and are then injected IP with 30 mg/kg calcein to label actively mineralizing bone. Four days later the same procedure is repeated. On the day of euthanization the mice are injected with a lethal dose of anesthetic, exsanguinated by cardiac puncture, and a contact x-ray captured before rigor mortis sets in. The skull, humeri, thoracic spine, and left femur and tibia are carefully disarticulated, placed in sterile polyethylene tubes, and frozen at -80°C along with the serum from separated blood to await analyses. The lumbar vertebrae and right femur and tibia are removed and placed immediately into cold 4% paraformaldehyde, fixed overnight at 4°C , rinsed thoroughly, and transferred to sterile PBS prior to μCT scanning on the Skyscan 1172 and processing for histology

(3D) imaging of rodent bones. The Skyscan 1172 currently in use at our institution is equipped with an x-ray source of maximum power 10 W and 100 kV. A 10 megapixel camera, micro-positioning stage, and NRecon software enable scanning and 3D reconstruction of specimens measuring approximately $7.0 \times$

3.5 cm at a resolution of up to $8,000 \times 8,000$ pixels and a detection limit of $0.7 \mu\text{m}$ isotropic detail. A typical ROI selected for quantitative μCT analysis is identified in reference to an anatomical landmark to ensure reproducibility from one specimen to the next. This is particularly relevant when comparing mice carrying mutations that affect the longitudinal growth of bones through the growth plates with their wild-type counterparts. A convenient landmark for the upper limit of the ROI in the distal femur is the lower edge of the femoral condyles as they appear in transverse sections. Typically, at a resolution of $5 \mu\text{m}$ the scan will be extended through a stack of 300 sections to generate a volumetric picture of trabecular bone in the proximal femur from which quantitative data can be generated. Many of the architectural parameters that were previously derived from histomorphometric analyses of serial two-dimensional (2D) sections can now be measured directly from these 3D CT reconstructions. The parameters most frequently used to describe bone architecture are the ratio of bone volume to tissue volume (BV/TV), trabecular thickness (Tr.Th), separation (Tr.Sp), and number (Tr.N), as well as measurements of their orientation (structure model index [SMI]) and connectivity (trabecular bone pattern factor [TbPf]). Additional measurements of cortical width at several different regions of the diaphysis as well as measuring BMD using an appropriate phantom are useful indices of the predicted biomechanical strength of the bone. If the primary interest is trabecular bone, then similar information can be captured from a defined ROI in vertebral bone.

2.3 Secondary Screen for Pathogenetic Mechanisms

When screening RCS or other populations of mice for skeletal defects, such as those that have undergone chemical mutagenesis, only those showing a distinct phenotype on the μCT analysis are subjected to a labor-intensive secondary screen. In contrast, investigators who have generated a single targeted mutation in a suspected bone active gene should always undertake this step, regardless of the outcome of the primary screen. While the primary screen provides quantitative data on the relative amount and micro-architecture of

bone, it provides no information on non-mineralized tissue or cellular composition, both of which provide critical information on the pathogenetic mechanisms underlying a bone phenotype.

2.3.1 Undecalcified Histology

The same femur that was used for the μ CT scan is trimmed and processed for embedding in polymethylmethacrylate (PMMA) at low temperature for preservation of enzyme activity and for undecalcified histological analysis.³¹ Serial 2–5 μ m sections are cut on a rotary microtome such as the Leica RM2265 (Leica Microsystems), which is equipped with a tungsten-carbide knife. Sections cut at intervals throughout the block and stained with Von Kossa and counterstained with toluidine blue can be accurately matched to 2D μ CT images to corroborate the quantitative results. Von Kossa stains mineralized tissue black and distinguishes it from blue non-mineralized tissue, such as cartilage, osteoid, fibrous tissue, or bone marrow (Fig. 2.1b). Adjacent sections are stained with tartrate resistant acid phosphatase (TRAP) for multinucleate osteoclasts and their precursors, and with alkaline phosphatase (ALP) to identify osteoblasts and hypertrophic chondrocytes in the epiphyseal growth plates (Fig. 2.1d). Metachromatic staining with toluidine blue alone is also useful in immature bone specimens to distinguish the primary spongiosa bone that is deposited on cartilage cores (Fig. 2.1c). If the primary interest is growth plate or epiphyseal cartilage, then a Safranin O stain should also be used to identify proteoglycan. These histochemical stains provide valuable qualitative data on the cell and tissue composition of trabecular and cortical bone and the relationship between mineralized and non-mineralized tissues.

2.3.2 Histomorphometry

A detailed discussion of the applications and methodology for histomorphometry can be found in [Chap. 4](#) of this book while this discussion will be restricted to those analyses that form an integral part of a secondary phenotypic screen. Quantitative histomorphometric

data that are often required to corroborate the results from μ CT and routine histopathology analyses are the number of osteoblasts and osteoclasts per unit of bone surface. This requires a microscope equipped with a calibrated eyepiece micrometer, or reticle, that can accommodate object (cells) and distance (bone surface) measurements accompanied by an analytical software package such as Osteomeasure (OsteoMetrics Inc). The number of osteoclasts or osteoblasts per millimeter of bone surface (Oc.N/mm or Ob.N/mm) are quantified in a defined ROI, preferably corresponding to that used for the μ CT analyses. The same software can quantify the amount of bone laid down between the two consecutive fluorescent labels of calcein, which was injected intraperitoneally (IP) at a concentration of 30 mg/kg at 7 and 3 days prior to euthanization to mark actively mineralizing surfaces (Fig. 2.2). The tibia and several lumbar vertebrae are often isolated for this dynamic histomorphometric measurement as the processing differs from that used routinely for bone phenotyping.

2.3.3 Biochemistry

A more complete discussion of the applications and methodology for biochemical markers of bone disease can be found in [Chap. 6](#) of this book. The similarities between human and murine bone growth and metabolism has facilitated the development of scaled-down rodent biomarker assays for serum and urine based on those used for screening human populations. Tests that are included in a secondary bone screen are calcium, phosphate, ALP, parathyroid hormone (PTH), vitamin D (VitD), markers of osteoblast and osteoclast activity and type-1 collagen breakdown (CTX). Many of the early mutations exploring osteopenic bone disease were targeted directly or indirectly at components of the classic PTH/VitD axis and their effect on calcium and phosphate metabolism. It is therefore not surprising that PTH and VitD levels were the first to be analyzed along with calcium and phosphate in the systemic circulation of rodents undergoing a secondary bone screen. The anabolic action of PTH in bone, which led to its United States Food and Drug Administration (FDA) approval as a therapy for advanced osteoporosis, is

believed to be mediated through the Wnt signaling pathway.³² Abnormalities in histochemical staining of osteoblasts and osteoclasts in bone can be followed up with serum assays for many bone active growth factors and cytokines that are available commercially in kit form. These include FGFs, IGF-1, PDGF, EGF, VEGF, TGF beta, Interleukins 1 and 6, tumor necrosis factor alpha (TNF- α), osteoprotegerin (OPG), and RANK ligand. Needless to say, the number of assays performed is limited not only because of their high cost but also by the relatively small amount of serum from blood obtained by cardiac puncture at the time of euthanization.

2.3.4 Chemical Composition of Bone

Of increasing importance to the study of bone strength is its chemical composition. Historically the relationship between collagen and hydroxyapatite crystals has been examined at the ultrastructural level using electron microscopy^{33,34} and the composition of the mineral phase quantified using a variety of biochemical assays including atomic absorption spectroscopy. Calcium, phosphate, magnesium, and various trace elements are measured in bone ash that is dissolved in acid and diluted in a solution, that is aspirated and burned in an acetylene air flame at a temperature of up to 2,800°C. This is a rapid, sensitive, and specific method for quantifying the ratio of calcium to phosphate or for determining the presence of elements such as magnesium, aluminum, strontium, zinc, or others that might influence bone strength.³⁵ Applications of alternative, nondestructive technology to examine the relationship between collagenous and non-collagenous components of bone in situ are gaining in popularity, including Fourier transform infrared (FT-IR)³⁶ and Raman spectroscopy.^{37,38} Of particular interest is the development of methodology for transcutaneous Raman spectroscopy for use in live animals.³⁹

2.3.5 Biomechanical Testing

Alterations in bone morphology, micro-architecture, composition, and turnover that are identified in the

primary and secondary screens will ultimately impact on bone strength. A detailed discussion of the applications and methodology for biomechanical testing of trabecular and cortical bone strength is found in [Chap. 3](#) of this book. These tests are best performed in specialized biomechanical engineering labs where the instruments have often been purpose-built and there is an acquired expertise. As a nonexpert it is reasonably easy to identify the need for expert advice and collaboration on testing the biomechanical strength of a mutant bone. For example, the thin femoral cortices demonstrated on a μ CT screen of adult FGFR3^{-/-} mice suggested the femoral diaphysis would be less resistant to loading and would fracture more readily in a three-point bending test.¹⁵ The hypothesis was validated in collaboration with the Buschmann team at Ecole Polytechnique who had developed the Mach-1 micro-mechanical tester marketed through Biosyntech Inc. (Laval, Quebec). A similar micro-mechanical tester from Instron Corp. (Canton, MA) was used to determine the relative resistance to compressive force of trabecular bone in the vertebrae of inbred strains of mice with differing susceptibility to fluorosis.⁴⁰

2.4 Tertiary Screen for Molecular Mechanisms

In situ analysis of bone cell function using immunohistochemical localization of proteins or in situ hybridization of RNA is technically challenging and labor-intensive and is therefore not commonly included in a secondary screen. The assays do, however, provide extremely valuable information on the identity of cells contributing to the bone phenotype. Protocols have been developed in specialized labs for immunohistochemical analysis of undecalcified tissue⁴¹ while others prefer to perform immunostaining on decalcified specimens, which usually means processing another bone ([Fig. 2.2](#)).

2.4.1 Demineralization

To preserve the antigenicity of proteins and the integrity of RNA, bone should be demineralized slowly

in suspension in 4% ethylenediaminetetraacetic acid (EDTA) over a period of a few weeks at 4°C. A simple, but time-consuming mechanism is to wrap individual specimens in a fine cheesecloth pouch with a dental-floss closure that is used to suspend the pouches in a 10× volume/specimen of EDTA that is slowly agitated on a stirring plate. The frequency of changes and length of time in the EDTA will depend on the number and size of specimens as well as the age and species of the donor. For example, adult mouse long bones take up to 4 weeks for complete demineralization whereas a 1 cm core from an equine carpal bone takes up to 12 weeks before it yields to a needle-prick test for malleability. A variety of rapid demineralization protocols that use up to 20% EDTA with microwave treatment or 8% hydrochloric/formic acid have been developed for specific applications including clinical diagnostics using *in situ* hybridization and immunochemical analyses. While the rapid demineralization protocols are more convenient and less tedious they tend to compromise certain histochemical stains and also result in some loss of resolution in cellular structure. To maintain the full range of options for high-resolution histochemical, *in situ* hybridization and apoptosis labeling, and immunochemical staining that are needed to characterize a skeletal phenotype both plastic and paraffin embedding should be performed. Once the specimens are adequately demineralized, they can be embedded in paraffin using automated equipment in any high-quality fee-for-service facility located in most academic departments and centers.

2.4.2 Immunohistochemistry

The focus of a tertiary immunochemical screen for anabolic or catabolic markers will depend largely on the outcome of the initial histological screen on undecalcified specimens. For example, an apparent decrease in ALP staining along trabecular bone surfaces in association with a decrease in mineralized tissue and no change in TRAP staining suggests a primary defect in osteogenic cells. On the other hand, a similar osteopenic phenotype in association with no apparent change in ALP but increased TRAP staining warrants further examination of osteoclasts and their precursors. Of course these clear-cut discrepancies are the exception rather than the rule and an extensive analysis involving several markers is usually required. The

antibodies used in an immunochemical screen of histological sections of bone should be selected carefully on the basis of the role of target antigens and the protocols should contain adequate controls, such as pre-adsorbed antisera, to avoid false-positive results. With the current widespread access to commercial facilities for the rapid and cost-effective production of high-quality antisera to novel proteins, the use of *in situ* hybridization is often restricted to cases where the protein is extremely low in abundance due to low production levels or rapid turnover.

2.4.3 Bone Cell Culture *Ex Vivo*

The second arm of a tertiary bone screen involves *ex vivo* investigation of the cells that manufacture and maintain *in vivo* mineralized tissue in order to identify potential alterations in their growth, differentiation, and activity. These assays can be performed in any wet lab with tissue culture facilities and molecular biology expertise. However, the knowledge required for the isolation of primary cells from whole bone or bone marrow is best learned from a lab that specializes in these techniques. There are a few labs that are focused primarily on the isolation, *ex vivo* differentiation, and activity of osteoclasts and their precursors. If the primary bone phenotype is one of osteopetrosis rather than osteoporosis, then a lab specializing in the isolation and functional characterization of osteoclasts should be consulted. Given the current interest in regenerative and reconstructive medicine (see below) there are a growing number of labs in the engineering, health sciences, and the private sectors that are developing techniques for the isolation and *ex vivo* expansion of cells of the osteogenic lineage. Although there is no consensus on the best source of cells to study the process of bone formation *ex vivo*, one promising approach appears to be the use of bone marrow stromal cells (MSCs).⁴² MSCs are accessible in relatively large numbers from the long bones of mice and rats, have some capacity for self-renewal, and can be induced to differentiate down the osteogenic lineage. Their capacity for self-renewal renders them conducive to gene transfer *ex vivo*, for the purpose of controlled release of critical factors necessary to induce or maintain the differentiated phenotype when transplanted *in vivo* (www.cshprotocols.org August 2009). An alternative approach has been to

use mature cells although this is frequently hampered by their limited proliferative capacity and the tendency to dedifferentiate in culture.⁴³

Protocols for the harvest, culture, and *ex vivo* phenotypic analysis of cells of the osteogenic lineage were established in the 1960s, well in advance of the 1980s explosion in transgenic science. The ability to make direct comparisons between primary osteogenic cells harvested from wild-type mice and their genetically modified litter-mates has been largely responsible for the shift away from the use of immortalized and transformed cell lines such as MC3T3 and UMR. A comprehensive discussion of the characteristics of multi-potent bone marrow-derived MSCs and their stepwise transition to fully functional osteoblasts can be found in Aubin et al.⁴⁴ Two-dimensional cultures and the “bone nodule” assay have been used extensively to explore the molecular mechanisms that give rise to a particular *in vivo* bone phenotype. The skeletally mature FGFR3-deficient mouse is a good example, where the *in vivo* phenotype is primarily one of osteomalacia and osteopenia.¹⁵ The absence of any obvious alterations in circulating levels of PTH or VitD suggested a problem in the bone micro-environment, most probably at the level of the osteoblast. Whole bone marrow harvested from the femora and tibia was filtered to remove debris and obtain a single cell solution that was plated on tissue culture plastic to select for adherent MSCs, which were plated at high density to perform a classic “bone nodule” assay. The commitment of MSCs to mature bone-forming osteoblasts is monitored *ex vivo* using similar techniques as those for *in vivo* histological analyses including ALP staining as an early marker of osteoblast differentiation and von Kossa stain to identify the mineralized matrix. In the absence of FGFR3 the population of MSCs grew faster, as demonstrated by MTT assay and ALP staining, but failed to form as many mineralized nodules as the wild-type cells. This *ex vivo* assay effectively demonstrated that there was a fundamental flaw in the capacity of isolated FGFR3-deficient osteoblasts to deposit mineral in the matrix they produced, which correlated with the *in vivo* observations of osteomalacia and osteopenia. Subsequent experiments would typically involve comparative microarray to identify differentially expressed genes and the use of analytical software such as Ingenuity Pathways® to identify biologically relevant gene networks. A more detailed description of the use of 3D culture of MSCs for *ex vivo* studies of bone formation follows under the heading of bone regeneration and repair.

2.5 Phenotyping Skeletal Regeneration and Repair

In developed countries, the average age of the population will continue to rise over the next two decades as the “baby boomers” currently in their fifth to seventh decades continue to age and their average life expectancy continues to increase with technological advancements in the health-care industry.⁴⁵ Bone mass normally declines in the fourth decade, thus placing individuals at increased risk to sustain a fracture, but they also become susceptible to failed union of those fractures as a consequence of an age-related decline in the capacity of tissue to repair itself.^{46,47} The reader is referred to Chap. 11 of this book for a detailed discussion of the mechanisms that have been proposed to account for age-related changes in bone regeneration which include a decrease in the availability of progenitor cells and in their ability to differentiate into bone-forming osteoblasts. As a consequence, the surgical reconstruction of fractures with hardware and the fixation of implants used in joint replacement are severely compromised in elderly patients. The result is an increase in patient morbidity and mortality, an escalation of the economic, personal, and social burdens associated with prolonged hospitalization and assisted home care, as well as reduced mobility and access to public spaces by our increasingly aged population.⁴⁸ These alarming facts emphasize the need to expedite research into regenerative medicine for the skeleton, to improve the quality of life of the aging population, and to decrease the economic burden associated with skeletal disease.

2.6 Bone Reconstruction in Clinical Practice

Therapeutic options for bone reconstruction are currently limited to rudimentary bone-grafting techniques with autogenous or allograft bone and single-dose intra-operative protein-based therapies.⁴⁹ Autogenous bone harvest from a remote site at the time of surgery that contains functional cells and matrix is preferred for grafting due to its superior osteo-inductive capability. Major drawbacks to this approach are the limited tissue supply and the high incidence of morbidity associated with bone harvest. An alternative approach is to use sterilized, devitalized allograft bone harvested

from cadaveric sources Allograft bone is more readily available but it has poor osteo-inductive capability, which leads to graft failure. Augmentation of allograft bone with vascularized fibular grafts⁵⁰ and adjuvant bone morphogenetic proteins (BMPs), to stimulate the recruitment and differentiation of endogenous osteogenic cells, have met with limited success in promoting integration of the graft with host bone.⁴⁹ Although these approaches can work well in some younger individuals, they are certainly not suitable for older patients who have structurally weak bones and a limited availability of endogenous MSCs and biologic factors for tissue repair.⁵¹ A promising approach for the “assisted” repair of bones under these and other poor healing conditions is transplantation of scaffolds pre-seeded with bone-forming cells and carrying bone anabolic agents, all of which require *in vivo* validation in an appropriate animal model.^{52,53}

2.7 Preclinical Animal Models

One approach that is gaining momentum is to use genetically defined mice, previously characterized with age-related bone phenotypes, to examine the efficacy of tissue-engineering strategies to induce regeneration and repair of surgically induced defects. However, mice are often too small to perform the surgical procedures such as an osteotomy with rigid fixation with any degree of consistency even when the hardware is custom-made. Rats are more than ten times the size of mice and can therefore be used for these complex orthopedic interventions to model fracture nonunion using instruments and hardware similar to that used for clinical applications. Like inbred mice, inbred rats offer the combined advantages of low cost, ease of access, extensive characterization, and genetic uniformity. Recent advances in rat genetics and genomics, together with a vast literature accumulated over a century on the physiology and pharmacology of the laboratory rat, predict that these animals will be used with increasing frequency for *in vivo* proof-of-concept studies.⁵⁴ In this context, the FDA guidelines recommend the use of the ovariectomized (OVX) rat model for the evaluation of new therapeutic agents for postmenopausal osteoporosis.⁵⁵ Surgically induced defects in the long bones of rats are gaining wide popularity to model bone healing under a variety of circumstances.⁵⁶⁻⁵⁸

2.8 Bone Tissue Engineering

2.8.1 Smart Scaffolds

Native bone is a nanocomposite material with a 3D hierarchical structure. It is composed of a largely inorganic phase dispersed in an oriented collagen matrix. Bone serves not only as a functional skeletal unit but also as an innate bio-incubator for cells that produce both matrix proteins and soluble factors required for renewal and repair of the scaffold.³⁴ The organic and inorganic components of bone exhibit nano- and microscale features believed to be important for the healing cascade.⁵⁹ It is thought that these features should be incorporated into implantable materials in order to control biological activity at the implant–bone interface. Controlling the interface, as well as the composition of the core scaffold structure itself, will result in improved mechanical strength and enhanced osteogenic function of the cellular component.⁶⁰ Advances in materials fabrication processes have enabled the manufacture of synthetic scaffolds that resemble bone in their structural hierarchy of nano- and microscale features. Synthetic bone analogues with useful mechanical properties and reproducible micro- and nano-sized features are relatively easy to fabricate from calcium phosphate and porous coralline ceramics for use in orthopedic applications. They can be used to deliver exogenous MSCs to the site of bone injury and their surfaces can be further functionalized with proteins that are conducive to the replication and differentiation of these cells into bone-forming osteoblasts. These microporous scaffolds made from biologic substrates, as well as those derived synthetically from degradable polymers or glass (Bioglass®), are easy to fabricate with reproducible structure and mechanical properties⁵² and have been approved for clinical use. However, their early promise for clinical applications has been limited by their resistance to degradation and replacement over time with mechanically and biologically functional, mineralized tissue, which is the primary objective of bone tissue engineering. In an attempt to overcome this shortcoming, porous ceramics loaded with bioactive agents for subsequent controlled release *in vivo* have been developed to allow for controlled resorption and replacement by native bone.⁶¹ These bone substitutes have significant advantages over bio-inert allografts, which include the capacity

for neo-vascularization and an extended surface area arising from their nanocrystallinity that is available for modification. Incorporation of microsensors into the 3D macroporous scaffolds would enable real-time monitoring of biological information such as pH, protein binding, oxygen, and growth factor availability.⁶² All of these factors will impact on the differentiation of precursor cells into osteoblasts and their subsequent capacity to manufacture new bone matrix. “Sense and Response Systems” can be programmed to record this biological information from the micro-environment and respond with the automated delivery of drugs and therapeutic agents to expedite bone healing.

Native collagen gels represent an alternative, biologically relevant scaffold that can be reconstituted *ex vivo* to encase viable cells for subsequent implantation in a bone defect. Dilute solutions of type-I collagen produce gels within minutes by the process of “fibrillogenesis” to form 3D lattices of collagen fibrils that self-assemble into a mesh that entraps cells and a large volume of fluid (>99%). To overcome the mechanical weakness of the hydrated gel, a novel process was developed that exploits the inherent property of collagen to release fluid when subjected to unconfined compression.⁶³ The end result of this compression yields a 3D tissue-like construct with useful mechanical properties and viable osteogenic cells⁶⁴ that can be implanted *in vivo*.⁶⁵ This scaffold has the obvious advantages of ultrarapid engineering compared with conventional cell-seeded collagen gels and, unlike synthetic polymers, will be resorbed and replaced with native bone.⁶⁶ Their ultimate success will be dependent on their physical properties, on “contingency” factors required to drive osteogenesis, and on robust phenotyping protocols, such as those described above, to evaluate their functional impact on bone formation *in vivo*.

2.8.2 Surgical Models to Study Bone Healing

A variety of surgical modifications of the bones of mice, rats, and rabbits have been developed in the laboratory to model fracture repair relying on the generation of a critical-sized defect, fixed internally or externally, which will not heal in the absence of adjunct therapy.⁶⁷⁻⁶⁹ This critical-sized osteotomy to model fracture nonunion is technically challenging in the rat. A 15 mm lateral

incision is made and the subcutaneous tissue carefully separated to expose the femur from the lateral femoral condyle proximally to the third trochanter. A custom polyethylene plate manufactured at the McGill Institute for Advanced Materials is aligned to span the mid-femoral diaphysis and attached to the bone using four 1.2 mm threaded Kirshner wires. A segment of bone measuring 1–5 mm, depending on the application, is then removed using an oscillating saw. Although attempts have been made to generate this nonunion with stable fixation model in mice, it is difficult to generate consistently and reproducibly. For this reason smaller drill-hole and window defects, which will eventually heal spontaneously over time, have been developed to study both trabecular and cortical bone regeneration.^{70,71} A small incision is made in the skin on the anterior aspect of the femur at the mid-diaphysis and the muscles splayed to expose the bone surface. One or two (window) overlapping full-thickness defects per femur are drilled through the cortex into the bone marrow cavity using a 1 mm dental burr with continuous saline irrigation to prevent thermal necrosis of the bone margins, and a jig to ensure a consistent depth. Depending on the objective of the experiment to study early or late events in bone healing the animals are maintained for up to 4 weeks post operation. Another model that is reasonably simple to generate in mouse femurs to investigate implant fixation under adverse conditions such as osteopenia is a modification of a classic technique used originally in 30 kg dogs. A 3 mm incision is made from the dorsal aspect where the femoral head joins the pelvic bone. The muscle insertion on the greater trochanter is then dissected free and the hip adducted to expose the piriformis fossa. A 25 gauge needle is inserted into the femoral canal immediately medial to the greater trochanter. Therapeutic agents are then injected into the femoral canal prior to insertion of a biocompatible orthopedic device. This model has been modified as illustrated in Fig. 2.3 to examine the potential of MSC transplantation for assisted bone repair in patients with poor-quality bone.

2.8.3 Phenotyping Bone Regeneration and Repair

The terminal procedures and quantitative analyses of bone regeneration and repair are essentially the same as

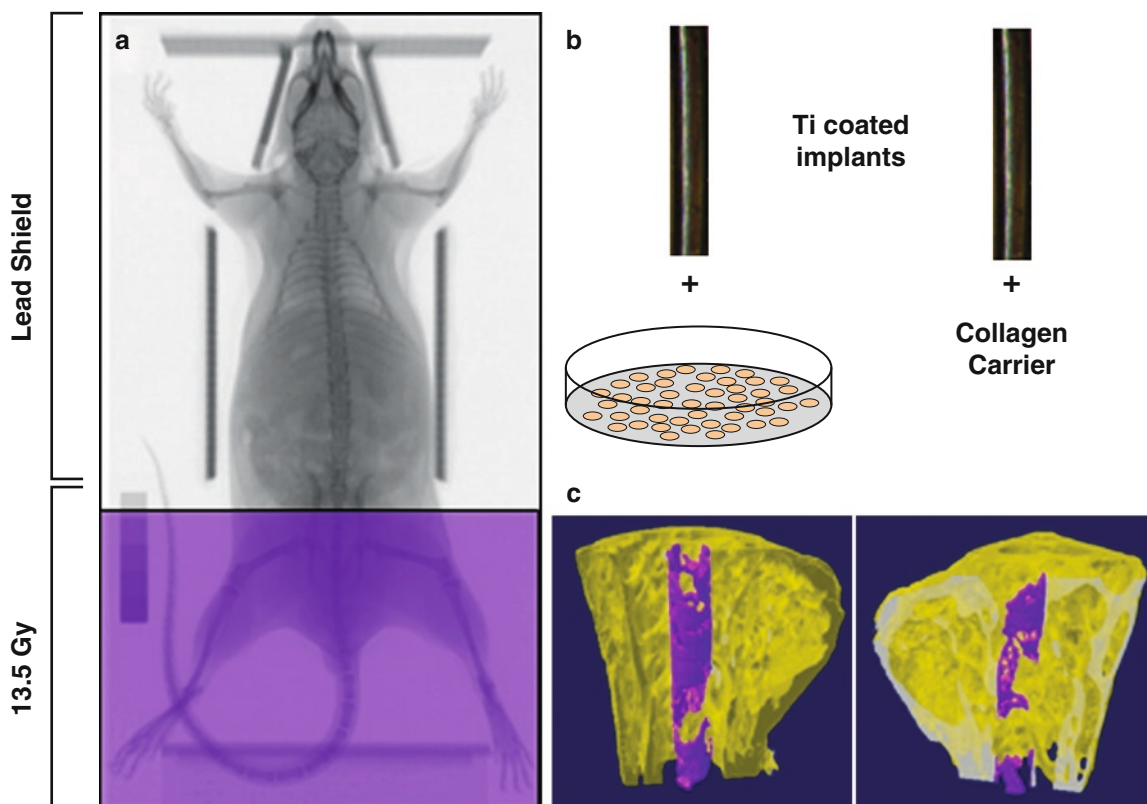


Fig. 2.3 Adult mouse sublethal irradiation and stem cell transplantation. Mice that have been characterized with defects in bone development or metabolism can be surgically modified to examine a variety of therapeutic interventions to promote bone regeneration. In this example, an osteopenic mouse was given a sublethal 13.5 Gy dose of irradiation to the lower limbs to kill endogenous bone marrow cells while a lead shield spared the depots in the upper body for hematopoiesis (a). MSCs from

a young healthy donor were transplanted into the right femur with a Ti-coated implant but only the implant with a collagen carrier was inserted into the left femur (b). The femurs were harvested after 6 weeks and the bones subjected to μ CT analysis, which showed that MSC transplantation stimulated significantly more new bone formation around the implant than was seen in the femur that received collagen alone (c)

those outlined above for the primary and secondary screens, with minor modifications. The animals are anesthetized with isoflurane, exsanguinated by cardiac puncture, and the serum separated and stored at -80°C for the biomarker assays. In contrast to a comprehensive screen where the entire axial and appendicular skeleton is harvested, only the surgically modified bones are removed for analysis in bone regeneration experiments. An x-ray instrument inside the pathogen-free zone is highly recommended in order to monitor the repair process over time, which can extend over 12 weeks for the rat critical-sized defects. Selection of the area of interest for μ CT analyses is difficult in the drill-hole and window defects due to their irregularity and slight inter-animal variation in shape. BMD around implants and in cortical defects can be

assessed by comparing the μ CT scans with those of standard hydroxyapatite “phantoms” of known density. The quantitative microstructural data obtained from μ CT can be correlated with FT-IR analysis of its elemental composition and the ratio of matrix to mineral, and with the mechanical properties evaluated by micro-indentation.

The histological analysis of bone regeneration is frequently complicated by the difference in composition between the trabecular bone surrounding intra-femoral implants and the implant itself, or between bone in a window defect and the surrounding femoral diaphysis. These specimens should be embedded in a more rigid resin such as LR White, Spurr, or Epon in order to minimize tissue damage at the implant–bone interface or between dense cortical and fine trabecular

bone. The downside to these procedures, which are normally reserved for electron microscopy applications, is that the stringent processing and curing often destroy enzyme activity and the resin must be removed from the sections before performing immunohistochemistry. Calcein labeling in the region of bone repair is evaluated on unstained sections and bone, osteoid, and fibrous tissue on von Kossa/toluidine blue-stained sections. Residual cartilage in bone undergoing endochondral ossification is identified by Safranin O/fast green staining. Bone-forming surfaces are identified by ALP activity and type-I collagen immunoreactivity in osteoblasts, while active areas of resorption are identified by TRAP activity in osteoclasts. It is also important to determine the relative rates of cell proliferation, using BrdU or proliferating cell nuclear antigen (PCNA) immunohistochemistry, and apoptotic cell death using ApopTag or an equivalent assay. These assays are particularly relevant when using animal models in which heritable defects are linked to excessive or insufficient apoptosis in endochondral bone development.

2.8.4 *Ex Vivo Culture of MSCs in Scaffolds*

For tissue-engineering applications, MSCs are most commonly grown in 3D culture on biocompatible, biodegradable scaffolds that mimic the composition and architecture of bone tissue to more closely simulate the *in vivo* environment. However, adherent cells can also be cultured under conditions that simulate the micro-mechanical forces and fluid flow dynamics of the *in vivo* environment.⁷² Thus, critical factors that will influence the replication and differentiation of the cells, such as load duration, magnitude, and cycle, as well as the fluid flow rate and fluid composition, can be precisely controlled. Much of the work aimed at developing effective scaffolds to promote bone formation *in vivo* has been driven by *ex vivo* studies that examine the response of isolated anabolic and catabolic cells to different chemical formulations.^{61,73-75} In addition to their chemical composition, an extensive literature documents the critical importance of surface topography in guiding the attachment, movement, and differentiation of osteogenic cells to scaffold materials during bone formation. It has been demonstrated that surface morphology is more important than surface

chemistry in promoting bone formation *in vivo*^{76,77} and inducing MSC differentiation *in vitro*.⁷⁸ In fact, it could be argued that the culture of stem cells can theoretically be optimized simply through modification of the nano- and micro-topography of the surface on which they are grown. These studies have been facilitated by the development of nondestructive assays such as AlamarBlue® to monitor the metabolic activity of cells growing in 3D scaffolds in the presence or absence of soluble factors over extended periods of time. At the termination of the experiment, the cell-seeded scaffolds are fixed in 4% paraformaldehyde and subjected to similar phenotyping protocols as have been described for native bone in the preceding sections. The process starts with μ CT quantification of mineral content followed by histological and ultrastructural assessment of the cells and matrix. The composite material generated by the *in vitro* culture system can also be subjected to FT-IR combined with x-ray diffraction to provide critical chemical and structural information on the calcium phosphate mineral deposited by the cells in the scaffold. Nano-indentation with the Mach-1 micro-mechanical tester can be used to measure the properties of the cell-seeded dense collagen scaffolds in much the same way as shown previously for articular cartilage. These data complement ultrastructural, chemical, and gene expression studies as they are performed in tissue samples.

2.9 Summary

Most academic institutions with extensive translational research programs that rely on the use of animal models of human disease have developed comprehensive services for biochemical analysis of body fluids, live animal imaging, soft tissue harvest, and processing and microscopic analysis. In parallel with the growth in transgenic science over the past two decades there has been a parallel increase in core facilities with the instrumentation and technical support for mineralized tissue analyses. These cores have enabled researchers with expertise in bone development and metabolism and an interest in bone phenotyping to develop customized protocols for the research community at large. The preceding paragraphs have described in detail a comprehensive phenotyping platform that was developed from experience accumulated over a decade characterizing

the skeletons of mice with targeted gene mutations and those generated through mutagenesis screens. The knowledge gained from this skeletal phenotyping platform is now being applied to address the changing needs of the research community for assessment of bone regeneration, fracture repair, and implant fixation.

Acknowledgments This work was supported in part by grants from the Canadian Institutes of Health Research, Genome Québec, the Fonds de la recherche en sante Quebec sponsored Réseau de recherché en transgénèse du Québec, and the Réseau de recherche en santé buccodentaire et osseuse. Dr. C. Gao is a scholar of the MENTOR Strategic Training in Health Research program. The authors thank Ailian Li, Wei Li, and Huifen Wang for their invaluable assistance with the mouse phenotyping work and Dr. J. Seuntjens of the Medical Physics Unit, McGill University, for collaboration with the mouse irradiation studies.

References

- Jaenisch R. Mammalian neural crest cells participate in normal embryonic development on microinjection into post-implantation mouse embryos. *Nature*. 1985;318:181-183.
- Thomas K, Capecchi M. Site-directed mutagenesis by gene targeting in mouse embryo-derived stem cells. *Cell*. 1987; 51:503-512.
- Fortin A, Diez E, Henderson J, Mogil J, Gros P, Skamene E. The AcB/BcA recombinant congenic strains of mice: strategies for phenotype dissection, mapping and cloning of quantitative trait genes. *Novartis Found Symp*. 2007;281: 141-153.
- Rivadeneira F, Consortium GFfO. Twenty bone mineral-density loci identified by large-scale meta-analysis of genome-wide association studies. *Nat Genet*. 2009;41:1199-1206.
- Miller P, Zapalowski C. Bone mineral density measurements. In: Goltzman D, ed. *The Osteoporosis Primer*. Cambridge: Cambridge University Press; 2000:262-276.
- Klein R, Mitchell S, Phillips T, Belknap J, Orwoll E. Quantitative trait loci affecting peak bone mineral density in mice. *J Bone Miner Res*. 1998;13:1648-1656.
- Lim L, Hoeksema L, Sherin K, Committee APP. Screening for osteoporosis in the adult US population: ACPM position statement on preventative practice. *Am J Prev Med*. 2009;36: 366-375.
- Griffith J, Genant H. Bone mass and architecture determination: state of the art. *Best Pract Res Clin Endocrinol Metab*. 2008;22:737-764.
- Richards J, Kavvoura F, Rivadeneira F, GFfO Consortium. Collaborative meta-analysis: association of 150 candidate genes with osteoporosis and osteoporotic fractures. *Ann Int Med*. 2009;151:528-537.
- Karsenty G. Transcriptional control of skeletogenesis. *Annu Rev Genomics Hum Genet*. 2008;9:183-196.
- Flenniken AM, Osborne L, Anderson N, Disease CfMH. A Gja1 missense mutation in a mouse model of oculodentodigital dysplasia (ODDD). *Development*. 2005;132:4375-4386.
- Ochotny N, Flenniken A, Owen C, et al. A point mutation in the V-ATPase subunit a3, R740S, uncouples ATP hydrolysis from proton transport and results in a dominant osteopetrosis phenotype. *J Bone Miner Res*. 2011 in press Feb 8. doi: 10.1002/
- Amizuka N, Davidson D, Liu H, et al. Signaling by fibroblast growth factor receptor 3 (FGFR3) and parathyroid hormone related protein (PTHrP) coordinate cartilage and bone development. *Bone*. 2003;34:13-25.
- Miao D, Liu H, Plut P, et al. Impaired endochondral bone development and osteopenia in Gli2 deficient mice. *Exp Cell Res*. 2003;294:210-222.
- Valverde-Franco G, Liu H, Davidson D, et al. Defective bone mineralization and osteopenia in young adult FGFR3-/- mice. *Hum Mol Genet*. 2004;13:271-284.
- Richard S, Valverde-Franco G, Tremblay GA, et al. Ablation of the Sam68 RNA-binding protein protects mice from age-related bone loss. *PLoS Genet*. 2005;1:e74-e84.
- Valverde-Franco G, Binette JS, Li W, et al. Defects in articular cartilage and early arthritis in fibroblast growth factor receptor 3 deficient mice. *Hum Mol Genet*. 2006;15:1783-1792.
- Deckelbaum RA, Majithia A, Booker T, Henderson JE, Loomis CA. The homeoprotein Engrailed-1 has pleiotropic functions in calvarial intramembranous bone formation and remodeling. *Development*. 2006;133:63-74.
- Lengner CJ, Steinman HA, Gagnon J, et al. Osteoblast differentiation and skeletal development are regulated by Mdm2-p53 signaling. *J Cell Biol*. 2006;172:909-921.
- Haston CK, Li W, Li A, Lafleur M, Henderson JE. Persistent osteopenia in adult Cftr-deficient mice. *Am J Respir Crit Care Med*. 2008;177:309-315.
- Rivas D, Li W, Akter R, Henderson J, Duque G. Accelerated features of age-related bone loss in Zmpste24 metalloproteinase-deficient mice. *J Gerontol*. 2009;10:1015-1024.
- Marquis J, Gros P. Genetic analysis of resistance to infections in mice: A/J meets C57BL/6J. *Curr Top Microbiol Immunol*. 2008;321:27-57.
- Beamer W, Donahue L, Rosen C, Baylink D. Genetic variability in adult bone density among inbred strains of mice. *Bone*. 1996;18:397-403.
- Turner C, Hsieh Y, Muller R, et al. Genetic regulation of cortical and trabecular bone strength and microstructure in inbred strains of mice. *J Bone Miner Res*. 2000;15:1126-1131.
- Turner C, Hsieh Y, Muller R, et al. Variation in bone biomechanical properties, microstructure, and density in BXH recombinant inbred mice. *J Bone Miner Res*. 2001;16:206-213.
- Rosen CJ, Dimal HP, Veraeault D, et al. Circulating and skeletal insulin like growth factor 1 (IGF-1) concentrations in two inbred strains of mice with different bone mineral densities. *Bone*. 1997;21:217-223.
- Delahunty K, Shultz K, Gronowicz G, et al. Congenic mice provide *in vivo* evidence for a genetic locus that modulates serum insulin-like growth factor-1 and bone acquisition. *Endocrinology*. 2006;147:3915-3923.
- D'Ascenzo M, Meacham C, Kirzman J, et al. Mutation discovery in the mouse using genetically guided array capture and resequencing. *Mamm Genome*. 2009;20:424-436.
- Colvin JS, Bohn BA, Harding GW, McEwen DG, Ornitz DM. Skeletal overgrowth and deafness in mice lacking fibroblast growth factor receptor 3. *Nat Genet*. 1996;12:390-397.

30. Deng C, Wynshaw-Boris A, Zhou F, Kuo A, Leder P. Fibroblast growth factor receptor 3 is a negative regulator of bone growth. *Cell*. 1996;84:911-921.
31. Chappard D, Palle S, Alexandre C, Vico L, Riffat G. Bone embedding in pure methyl methacrylate at low temperature preserves enzyme activities. *Acta Histochem*. 1987;81:183-190.
32. Williams B, Insogna K. Where Wnts went: the exploding field of Lrp5 and Lrp6 signaling in bone. *J Bone Miner Res*. 2009;24:171-178.
33. Boyde A, Jones S. Scanning electron microscopy of bone: instrument, specimen and issues. *Microsc Res Tech*. 1996;33:92-120.
34. Marks S, Odgren P. Structure and development of the skeleton. In: Bilezikian J, Raisz L, Rodan G, eds. *Principles of Bone Biology*. San Diego: Academic; 2002:3-16.
35. Lvov B. Fifty years of atomic absorption spectrometry. *J Anal Chem*. 2005;60:382-392.
36. Boskey A, Camacho N. FT-IR imaging of native and tissue-engineered bone and cartilage. *Biomaterials*. 2006;28:2465-2478.
37. Gentleman E, Swain R, Evans N, et al. Comparative materials differences revealed in engineered bone as a function of cell-specific differentiation. *Nat Mater*. 2009;8:763-770.
38. Goodyear S, Gibson I, Skakle J, Wells R, Aspden R. A comparison of cortical and trabecular bone from C57 Black 6 mice using Raman spectroscopy. *Bone*. 2009;44:899-907.
39. Schulmerich M, Cole J, Kreider J, et al. Transcutaneous Raman spectroscopy of murine bone *in vivo*. *Appl Spectrosc*. 2009;63:286-295.
40. Mousny M, Banse X, Wise L, et al. The genetic influence on bone susceptibility to fluoride. *Bone*. 2006;39:1283-1289.
41. Yang R, Davies C, Archer C, Richards R. Immunohistochemistry of matrix markers in Technovit 9100 New-embedded undecalcified bone sections. *Eur Cell Mater*. 2003;6:57-71.
42. Tamer E, Reis R. Progenitor and stem cells for bone and cartilage regeneration. *J Tissue Eng Regen Med*. 2009;3:327-337.
43. Hasegawa T, Oizumi K, Yoshiko Y, Tanne K, Maeda N, Aubin J. The PPARgamma-selective ligand BRL-49653 differentially regulates the fate choices of rat calvaria versus rat bone marrow stromal cell populations. *BMC Dev Biol*. 2008;8:1-12.
44. Aubin JE, Triffitt J. Mesenchymal stem cells and the osteoblast lineage. In: Bilezikian JP, Raisz LG, Rodan GA, eds. *Principles of Bone Biology*. 2nd ed. New York: Academic; 2002:59-81.
45. Johnell O, Kanis J. An estimate of the worldwide prevalence and disability associated with osteoporotic fractures. *Osteoporos Int*. 2006;17:1726-1733.
46. Shapiro F. Bone development and its relation to fracture repair. The role mesenchymal osteoblasts and surface osteoblasts. *Eur Cells Mater*. 2008;15:53-76.
47. Duque D. Bone and fat connection in aging bone. *Curr Opin Rheumatol*. 2008;20:429-434.
48. Pasco J, Sanders KM, Hoekstra FM, Henry MJ, Nicholson GC, Kotowicz MA. The human cost of fracture. *Osteoporos Int*. 2005;16:2046-2052.
49. Jones A, Bucholz R, Bosse M, et al. Recombinant BMP-2 and allograft compared with autogenous bone graft for reconstruction of diaphyseal tibial fractures with cortical defects. A randomized controlled trial. *J Bone Joint Surg Am*. 2006;88:1431-1441.
50. Friedrich J, Moran S, Bishop A, Wood C, Shin A. Free vascularized fibular graft salvage of complications of long-bone allograft after tumor reconstruction. *J Bone Joint Surg Am*. 2008;90:93-100.
51. Gruber R, Koch H, Doll B, Tegtmeier F, Einhorn T, Hollinger J. Fracture healing in the elderly patient. *Exp Gerontol*. 2006;41:1080-1093.
52. Khan Y, Yaszemski M, Mikos A, Laurencin C. Tissue engineering of bone: material and matrix considerations. *J Bone Joint Surg Am*. 2008;90:36-42.
53. Lee K, Chan C, Patil N, Goodman S. Cell therapy for bone regeneration: bench to bedside. *J Biomed Mater Res B Appl Biomater*. 2009;89:252-263.
54. Mashimo T, Serikawa T. Rat resources in biomedical research. *Curr Pharm Biotechnol*. 2009;10:214-220.
55. Whitfield J, Morley P, Willick G. Parathyroid hormone, its fragments and their analogs for the treatment of osteoporosis. *Treat Endocrinol*. 2002;1:175-190.
56. Herbenick M, Sprott D, Still H, Lawless M. Effects of a cyclooxygenase 2 inhibitor on fracture healing in a rat model. *Am J Orthop*. 2008;37:133-137.
57. Miettinen S, Jaatinen J, Peltari A, et al. Effect of locally administered zoledronic acid on injury-induced intramembranous bone regeneration and osseointegration of a titanium implant in rats. *J Orthop Sci*. 2009;14:431-436.
58. Boerckel J, Dupont K, Kolambkar Y, Lin A, Guldberg R. *In vivo* model for evaluating the effects of mechanical stimulation on tissue-engineered bone repair. *J Biomech Eng*. 2009;131:084502:1-5.
59. Ma D, Guan J, Normandin F, et al. Multifunctional nano-architecture for biomedical applications. *Chem Mater*. 2006;18:1920-1927.
60. Dalby M, Gadegaard N, Tare R, et al. The control of human mesenchymal cell differentiation using nanoscale symmetry and disorder. *Nat Mater*. 2007;6:997-1003.
61. Ibasco S, Tamimi F, Meszaros R, et al. Magnesium-sputtered titanium for the formation of bioactive coatings. *Acta Biomater*. 2009;5:2338-2347.
62. Harvey E, Henderson J, Vengallatore S. Nanotechnology and bone healing. *J Ortho Trauma*. 2010;24:S25-S30.
63. Brown R, Wiseman M, Chuo C, Cheema U, Nazhat S. Ultrarapid engineering of biomimetic materials and tissues: fabrication of nano- and microstructures by plastic compression. *Adv Funct Mater*. 2005;15:1762-1770.
64. Bitar M, Brown R, Salih V, Kidane A, Knowles J, Nazhat S. Effect of cell density on osteoblastic differentiation and matrix degradation of biomimetic dense collagen scaffolds. *Biomacromolecules*. 2008;9:129-135.
65. Mudera V, Morgan M, Cheema U, Nazhat S, Brown R. Ultra-rapid engineered collagen constructs tested in an *in vivo* nursery site. *J Tissue Eng Regen Med*. 2007;1:192-198.
66. Buxton P, Bitar M, Gellynck K, et al. Dense collagen matrix accelerates osteogenic differentiation and rescues the apoptotic response to MMP inhibition. *Bone*. 2008;43:377-385.
67. Bonnarens F, Einhorn T. Production of a standard closed fracture in laboratory animal bone. *J Orthop Res*. 1984;2:97-101.

68. Palomares K, Gleason R, Mason Z, et al. Mechanical stimulation alters tissue differentiation and molecular expression during bone healing. *J Orthop Res*. 2009;27:1123-1132.
69. Fu L, Tang T, Miao Y, Hao Y, Dai K. Effect of 1, 25-dihydroxy vitamin D3 on fracture healing and bone remodeling in ovariectomized rat femora. *Bone*. 2009;44:893-898.
70. Karp J, Sarraf F, Shoichet M, Davies J. Fibrin-filled scaffolds for bone-tissue engineering: an *in vivo* study. *J Biomed Mater Res A*. 2004;71:162-171.
71. Nagashima M, Sakai A, Uchida S, Tanaka S, Tanaka M, Nakamura T. Bisphosphonate (YM520) delays the repair of cortical bone defect after drill-hole injury by reducing terminal differentiation of osteoblasts in the mouse femur. *Bone*. 2005;36:502-511.
72. Majd H, Wipff P, Buscemi L, et al. A novel method of dynamic culture surface expansion improves mesenchymal stem cell proliferation and phenotype. *Stem Cells*. 2009;27:200-209.
73. Jabbarzadeh E, Starnes T, Khan Y, et al. Induction of angiogenesis in tissue-engineered scaffolds designed for bone repair: a combined gene therapy transplantation approach. *Proc Natl Acad Sci USA*. 2008;105:11099-11104.
74. Rosa A, de Oliveira P, Beloti M. Macroporous scaffolds associated with cells to construct a hybrid biomaterial for bone tissue engineering. *Expert Rev Med Devices*. 2008;5:719-728.
75. LeNihouannen D, Komarova S, Gbureck U, Barralet J. Bioactivity of bone resorptive factor loaded on osteoconductive matrices: stability post-dehydration. *Eur J Pharm Biopharm*. 2008;70:813-818.
76. Hacking S, Zuraw M, Harvey E, Tanzer M, Krygier J, Bobyn J. A physical vapor deposition method for controlled evaluation of biological response to biomaterial chemistry and topography. *J Biomed Mater Res A*. 2007;82:179-187.
77. Hacking SA, Tanzer M, Harvey EJ, Krygier JJ, Bobyn JD. Relative contributions of chemistry and topography to the osseointegration of hydroxyapatite coatings. *Clin Orthop Relat Res*. 2002;405:24-38.
78. Hacking S, Harvey E, Roughly P, Tanzer M, Bobyn J. The response of mineralizing culture systems to microtextured and polished titanium surfaces. *J Orthop Res*. 2008;26:1347-1354.



<http://www.springer.com/978-0-85729-292-6>

Osteoporosis Research

Animal Models

Duque, G.; Watanabe, K. (Eds.)

2011, XIX, 196 p., Hardcover

ISBN: 978-0-85729-292-6